

# DUAL-GRATING DIELECTRIC ACCELERATORS DRIVEN BY A PULSE-FRONT-TILTED LASER\*

Y. Wei<sup>†</sup>, C. P. Welsch, Cockcroft Institute and University of Liverpool, UK  
 G. Xia, Cockcroft Institute and University of Manchester, UK  
 R. Ischebeck, M. Dehler, E. Ferrari, N. Hiller, Paul Scherrer Institute, Villigen, Switzerland  
 J. D. A. Smith, Tech-X UK Ltd, Sci-Tech Daresbury, Warrington, UK

## Abstract

Dielectric laser-driven accelerators (DLAs) can provide high accelerating gradients in the GV/m range due to their higher breakdown thresholds than metals, which opens the way to miniaturize our next-generation particle accelerator facility. However, the electron energy gain is limited by the short interaction length between the laser pulses and the electron bunch for previously reported DLAs. This paper numerically investigates the dual-grating DLAs driven by a pulse-front-tilted (PFT) laser which extends the interaction length and boosts the electrons energy gain. The optical system to generate the PFT laser beam is also studied in detail. By two-dimensional (2D) particle-in-cell simulations we show that such a PFT laser effectively increases the energy gain by more than 100% as compared to that of a normally incident laser beam.

## INTRODUCTION

Dielectric laser-driven accelerators (DLAs) utilizing the large electric fields from commercial laser systems to accelerate particles with high gradients, of the order of GV/m, have the potential to realize a particle accelerator ‘on a chip’. Grating-based structures proposed by Plettner et al. [1] are one of the candidates for DLAs. They can be mass-produced using available nanofabrication techniques due to their simpler structural geometry compared to other types of DLAs. This offers a far less expensive way to build high performance particle accelerators of much smaller size than conventional ones in the future. So far grating-based structures have been experimentally demonstrated the accelerating gradients of up to 300 MV/m [2], 690 MV/m [3] for relativistic electron acceleration and gradients of 25 MV/m [4] and 370 MV/m [5] for non-relativistic electron acceleration.

Geometry optimizations [1][6-8] have been carried out to maximize the accelerating gradient, thus resulting in the large energy gain for DLAs. However, previous DLAs studies were performed with a normally-incident laser beam. In this case the increase in electron energy is limited by the short interaction length between the laser pulses and the electron bunch. In this paper we explore the dual-grating DLAs driven by a PFT laser to extend the interaction length, thereby resulting in a great energy gain. As shown in Fig. 1, a PFT laser beam is introduced to interact with an electron bunch in a dual-grating structure. The tilt angle  $\gamma$  can be chosen to synchronously overlap an electron bunch with the laser pulse envelope so

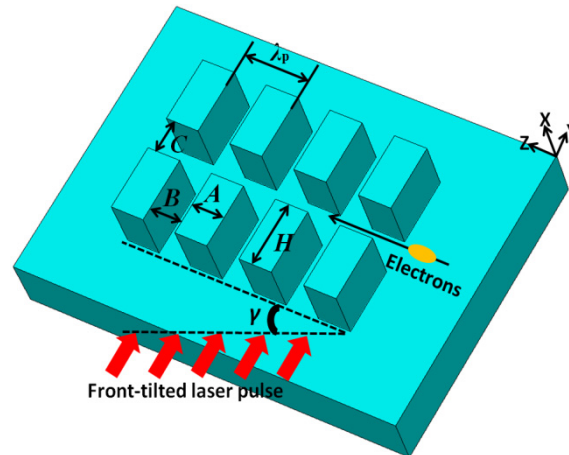


Figure 1: Schematic of a dual-grating structure illuminated by a PFT laser beam with a tilt angle of  $\gamma$ .  $\lambda_p$ ,  $A$ ,  $B$ ,  $C$ , and  $H$  represent grating period, pillar width, pillar trench, vacuum channel gap and pillar height, respectively.  $A + B = \lambda_p$  is selected for all simulations.

that the electrons obtain the largest energy gain.

## OPTICAL SYSTEM FOR THE PFT LASER

In this section, we discuss the optical system to generate the desired PFT laser. A PFT laser can be generated either by angular dispersion (AD) which causes different frequency components to propagate at different angles or by simultaneous spatial and temporal focusing (SSTF) in the absence of AD. SSTF has been demonstrated in Ref. [9] to generate a PFT laser beam with an ultrashort pulse duration of  $\sim 100$  fs at the focal region, but the waist radius is also focused to tens of  $\mu\text{m}$ , thereby limiting the energy gain for DLAs. Martinez et al. [10] showed that the PFT laser achieved by AD gives rise to pulse broadening and changing of the tilt angle as it moves away from a diffractive grating or prism. However, these distortion can be compensated for by using an imaging lens to transfer the image of a tilted pulse front on the diffraction grating into the dual-grating DLAs.

As shown in Fig. 2, our PFT setup consisting of a diffraction grating and an imaging lens. An incident laser beam experiences an angular dispersion when it is propagating through a diffraction grating. This means that different spectral components of a laser pulse travel in different directions after passing the diffraction grating. As a consequence, the laser pulse front is tilted by an angle  $\gamma$  whereas the phase fronts of the pulse are always perpendicular to the pulse propagation direction.

\* Work supported by the EU under grant agreements 289191, as well as the Cockcroft Institute core Grant No. ST/G008248/1.

<sup>†</sup> yelong.wei@cockcroft.ac.uk

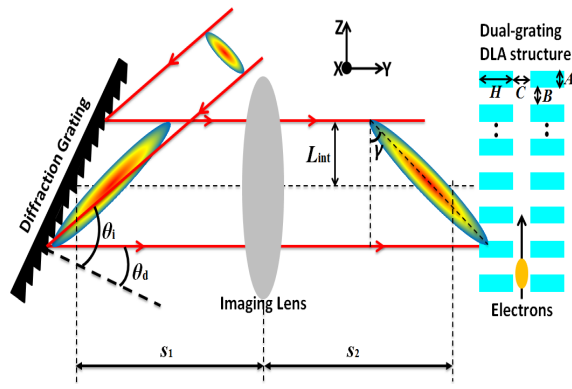


Figure 2: Diagram of a front-tilted laser pulse generated by a dedicated optical system.

The optical setup in Fig. 2 has been analyzed in Ref. [11] and accordingly the equations are listed:

$$\sin \theta_d = \frac{\lambda_0}{p} a, \quad (1)$$

$$\sin \theta_i = \frac{\lambda_0}{p} - \sin \theta_d, \quad (2)$$

$$s_1 = f(\sqrt{a} + 1), \quad (3)$$

$$s_2 = \frac{f s_1}{s_1 - f}, \quad (4)$$

$$a = \frac{p}{2\lambda_0} \sqrt{\frac{(\lambda_0)^2}{p^2(\tan \gamma)^4} + 4} - \frac{1}{2(\tan \gamma)^2}, \quad (5)$$

where  $\theta_i$  and  $\theta_d$  are incidence and diffraction angles, respectively,  $\lambda_0$  is laser wavelength,  $p$  is the grating period and  $f$  is the focal length of the imaging lens, and  $\gamma$  is the tilt angle for a pulse front.

The tilt angle between the pulse front and the direction  $z$  is given by [12]

$$\tan \gamma = pc = 1. \quad (6)$$

where  $p$  is the PFT factor and  $c$  is the speed of light. In order to synchronously overlap with relativistic electrons, the PFT angle  $\gamma$  equals to  $45^\circ$ , as described in Ref. [1].

When an incident laser pulse travels through the diffraction grating, the upper side of the pulse is diffracted by the grating earlier than the lower side of the pulse. This generates an optical path difference, which contributes to a front-tilted pulse close to the grating. Such a front-tilted pulse has the same pulse duration as the incident laser pulse. In this case, the pulse intensity and peak field remain constant. Then an imaging lens is used to transfer the front-tilted pulse at the plane with a distance of  $s_1$  to the plane with a distance of  $s_2$  from the lens. This imaging process does not generate any distortion for the front-tilted pulse. The imaged front-tilted pulse should be put close enough to the dual-grating structure in order to reduce the broaden effect [11]. In this

paper, the pulse duration is assumed to remain constant when it is introduced into the dual-grating DLAs.

Using such optical system, a PFT laser beam with a peak field of  $E_0$ , a waist radius of  $L_{\text{int}}$  and a local temporal duration of  $\tau_0$  can be generated. The mathematical expression for the electric field of such a PFT beam is:

$$E'_z = E_0 e^{-\left(\frac{z}{L_{\text{int}}}\right)^2} e^{-2 \ln 2 \left(\frac{t-pz}{\tau_0}\right)^2} \cos(\omega t - k_0 y + \phi_1), \quad (7)$$

where  $\omega$  is the angular frequency,  $k_0$  is the wave number and  $\phi_1$  is a phase term. When the electrons move at a speed of  $c$ , we can get  $t - pz = 0$ . So the electrons experience a Gaussian field along the channel centre:

$$E'_t = G_p e^{-\left(\frac{z}{L_{\text{int}}}\right)^2} \cos(\omega t - k_z z + \phi_2), \quad (8)$$

where  $G_p$  is the peak gradient,  $k_z = k_0/\beta$  is the longitudinal wave number and  $\phi_2$  is a phase term.

## PARTICLE-IN-CELL SIMULATION

In this section, we investigate the interaction between a front-tilted laser pulse and a Gaussian electron bunch in a 100-period quartz dual-grating structure with geometries:  $A = B = 0.50\lambda_p$ ,  $C = 0.50\lambda_p$ ,  $H = \lambda_p$ ,  $\lambda_p = 1 \mu\text{m}$ . The electron bunch employed in our simulations has a mean energy of 50 MeV, bunch charge of 0.1 pC, RMS length of 9  $\mu\text{m}$ , RMS radius of 10  $\mu\text{m}$ , normalised emittance of 0.2 mm mrad, and energy spread of 0.05%. Such an electron bunch can be achieved from future Compact Linear Accelerator for Research and Applications (CLARA) [13].

An input laser pulse with  $\lambda_0 = 1 \mu\text{m}$  wavelength,  $\Delta P = 7 \mu\text{J}$  pulse energy,  $\tau_0 = 100$  fs pulse duration, and  $w_r = 50 \mu\text{m}$  waist radius would generate an input peak field  $E_0 = 3$  GV/m. When such a laser pulse is normally used for illumination, the maximum electric field is still under the damage threshold for quartz structures [1]. In its co-moving frame, the electrons experience a Gaussian-

distributed temporal field  $E_t = G_p e^{-\left(\frac{z}{w_{\text{int}}}\right)^2}$  with a interaction length  $w_{\text{int}} = \left(\frac{1}{(w_r)^2} + \frac{2 \ln 2}{(c\tau_0)^2}\right)^{-0.5} = 22.7 \mu\text{m}$ , as described in Ref. [8]. Integrating  $E_t$  with a peak gradient of  $G_p = 1.0$  GV/m results in a maximum energy gain of  $\Delta E_m = 40$  keV, which can be used to calculate the loaded gradient for subsequent analysis.

The same laser parameters are used for optical system as shown in Fig. 2 to generate a front-tilted pulse with an ultrashort pulse duration of  $\tau_0 = 100$  fs and tilt angle of  $\gamma = 45^\circ$ . A grating groove density of  $n = 1200$  line/mm ( $p = 0.83 \mu\text{m}$ ) is used firstly, substituting Eq. (6) into Eqs. (5), (1) and (2), we can derive that  $\theta_i = 39.3^\circ$  and  $\theta_d = 34.5^\circ$ . A long focal length of  $f = 150$  mm is chosen to reduce the imaging distortion [11] for tilt front. According to Eqs. (3) and (4), we can obtain that  $s_1 = 253.0$  mm and  $s_2 = 368.5$  mm. Based on the calculated

path difference, the waist radius for a front-tilted pulse is 94  $\mu\text{m}$ . Combining with Eq. (6), we can get the interaction length  $L_{\text{int}} = 94/\sqrt{2} = 66.5 \mu\text{m}$ . Then Eq. (7) is used to mathematically model such a front-tilted pulse for our 2D particle-in-cell simulation. When such a front-tilted pulse propagates through the dual-grating structure to interact with the electron bunch, the maximum energy gain is  $\Delta E'_m = 84 \text{ keV}$  when  $G_p = 1.0 \text{ GV/m}$  is used.

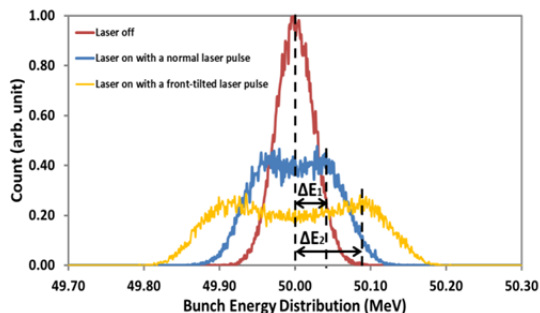


Figure 3: Bunch energy distribution for the cases of laser-off (red line), laser-on with a normal laser (blue line) and laser-on with a front-tilted laser (yellow line).

In our 2D particle-in-cell simulations, those electrons travelling through the quartz structure suffer significant energy loss due to collisional straggling [14] in the dielectrics, so only the electrons modulated by the laser field in the vacuum channel are used for our calculations. It is found that about 2% of the 50 MeV bunch is transmitted through the vacuum channel gap of 0.5  $\mu\text{m}$ . Figure 3 shows that the bunch energy distribution for modulated electrons with the laser off and on. It is obvious that the energy spectrum has a double-peaked profile after laser-bunch interaction, which agrees well with the reported results [2][8]. The maximum energy gain is  $\Delta E_1 = 42 \pm 5 \text{ keV}$  for normal laser illumination while it is  $\Delta E_2 = 90 \pm 11 \text{ keV}$  for the PFT laser illumination. This corresponds to maximum loaded gradients of  $1.05 \pm 0.13 \text{ GV/m}$  and  $1.07 \pm 0.13 \text{ GV/m}$ , respectively. It is found that both schemes have the similar loaded gradient but the PFT laser generates a double energy gain than a normal laser.

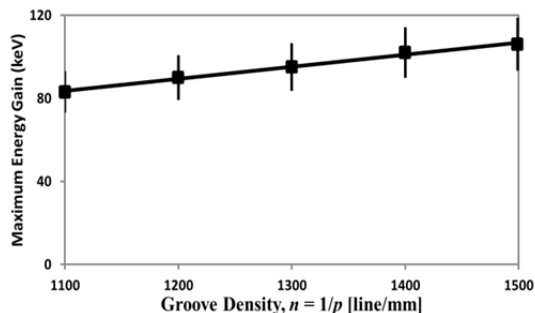


Figure 4: Numerically computed energy gain with different grating groove densities.

Later, we study the relationship between the computed maximum energy gain and the groove density of the diffraction grating which strongly affects the parameters of  $\theta_i$ ,  $\theta_d$ , and  $L_{\text{int}}$ , as shown in Eqs. (1) to (5). Figure 4

shows that the maximum energy gain linearly increases with a larger groove density. Due to limitation of Eq. (2), the groove density should be smaller than 1500 line/mm. So the maximum groove density is chosen as 1499 line/mm, corresponding to a maximum energy gain of  $106 \pm 13 \text{ keV}$ . This means that a PFT laser can effectively increase the energy gain by more than 100% as compared to a normal laser beam.

## CONCLUSION

This paper presented results from numerical studies into dual-grating DLAs driven by a PFT laser using the VSIM simulation code. It was shown that this setup can extend the interaction length between laser and beam, thereby boosting the energy gain as compared to conventionally driven DLAs. An overview of the required optical system to generate the desired PFT laser beam with an ultrashort pulse duration of 100 fs was also presented.

Detailed investigations into electron beam acceleration and transmission for the specific case of a grating groove density  $n = 1200 \text{ line/mm}$  were also presented. It was found that the maximum gradient remained unchanged, but that the energy gain is effectively increased for PFT laser illumination as compared to normal illumination.

By increasing the grating groove density and hence the improvements on the energy gain can be expected. It was shown that a groove density of 1499 line/mm can generate a maximum energy gain of  $106 \pm 13 \text{ keV}$ , which is more than double of energy gain achieved from a normal laser illumination. In addition, a larger laser waist radius and structure periods can boost the interaction length to 1 mm in principle, resulting in an energy gain of 1 MeV from the PFT laser illumination.

## ACKNOWLEDGEMENT

We would like to thank Dr. Steven Jamison for many useful discussions.

## REFERENCES

- [1] T. Plettner, *et al.*, *Phys. Rev. ST Accel. Beams* 9, 111301 (2006).
- [2] E. A. Peralta, *et al.*, *Nature* 503,91(2013).
- [3] K. P. Wootton, *et al.*, *Opt. Lett.*, 41, 2696 (2016).
- [4] J. Breuer and P. Hommelhoff, *Phys. Rev. Lett.* 111, 134803 (2013).
- [5] K. J. Leedle, *et al.*, *Opt. Lett.* 40, 4344 (2015).
- [6] A. Aimidula, *et al.*, *Phys. Plasmas* 21, 023110 (2014).
- [7] A. Aimidula, *et al.*, *Nucl. Instrum. Methods. Phys. Res., Sect. A* 740, 108 (2014).
- [8] Y. Wei, *et al.*, *Phys. Plasmas* 24, 023102 (2017).
- [9] M. E. Durst, *et al.*, *Opt. Commun.* 281, 1796 (2008).
- [10] O. Martinez, *Opt. Commun.* 59, 229 (1986).
- [11] J. Fülöp, *et al.*, *Opt. Express* 18, 12311 (2010).
- [12] S. Akturk, *et al.*, *Opt. Express* 12, 4399 (2004).
- [13] J. A. Clarke, *et al.*, *J. Instrum.* 9, T05001 (2014).
- [14] C. Warner III and F. Rohrlich, *Phys. Rev.* 93, 406(1954).